



HHS Public Access

Author manuscript

J Immunol. Author manuscript; available in PMC 2016 August 01.

Author Manuscript

Author Manuscript

Author Manuscript

Author Manuscript

Published in final edited form as:

J Immunol. 2015 August 1; 195(3): 1182–1190. doi:10.4049/jimmunol.1500348.

TGF- β -dependent dendritic cell chemokinesis in murine models of airway disease

Mitsuo Hashimoto^{*}, Haruhiko Yanagisawa^{*}, Shunsuke Minagawa^{*}, Debasish Sen^{*}, Royce Ma^{*}, Lynne A. Murray[§], Ping Tsui[§], Jianlong Lou[†], James D. Marks[†], Jody L. Baron[‡], Matthew F. Krummel^{*}, and Stephen L. Nishimura^{*,¶}

^{*}Department of Pathology, University of California, San Francisco, CA

[†]Department of Anesthesia and Perioperative Care, University of California, San Francisco, CA

[‡]Department of Medicine, University of California, San Francisco, CA

[§]Respiratory, Inflammation and Autoimmunity, MedImmune, Gaithersberg, MD and Cambridge, UK

Abstract

Small airway chronic inflammation is a major pathologic feature of chronic obstructive pulmonary disease (COPD) and is refractory to current treatments. Dendritic cells (DCs) accumulate around small airways in COPD. DCs are critical mediators of antigen surveillance and antigen presentation and amplify adaptive immune responses. How DCs accumulate around airways remains largely unknown. We use 2-photon DC imaging of living murine lung sections to directly visualize the dynamic movement of living DCs around airways in response to either soluble mediators (IL-1 β) or environmental stimuli (cigarette smoke or TLR3 ligands) implicated in COPD pathogenesis. We find that DCs accumulate around murine airways primarily by increasing velocity (chemokinesis) rather than directional migration (chemotaxis) in response to all three stimuli. DC accumulation maximally occurs in a specific zone located 26-50 μ m from small airways, which overlaps with zones of maximal DC velocity. Our data suggest that increased accumulation of DCs around airways results from increased numbers of highly chemokinetic DCs entering the lung from the circulation with balanced rates of immigration and emigration. Increases in DC accumulation and chemokinesis are partially dependent on *ccr6*, a crucial DC chemokine receptor, and fibroblast expression of the integrin $\alpha v\beta 8$, a critical activator of TGF- β . $\alpha v\beta 8$ -mediated TGF- β activation is known to enhance IL-1 β -dependent fibroblast expression of the only known endogenous *ccr6* chemokine ligand, *ccl20*. Taken together, these data suggest a mechanism by which $\alpha v\beta 8$, *ccl20* and *ccr6* interact to lead to DC accumulation around airways in response to COPD-relevant stimuli.

Introduction

Chronic obstructive pulmonary disease (COPD) is the third leading cause of death in the United States (1). Chronic inflammation surrounding small airways is refractory to currently

[¶]Stephen L. Nishimura, MD, SFGH/UCSF, Bldg 3/Rm 211, 1001 Potrero Ave., San Francisco, CA 94110, Phone (415) 206-5906 Fax (415) 206-5988, stephen.nishimura@ucsf.edu.

available therapies and is a major contributing factor leading to obstructive pathophysiology (2, 3). New therapies may be developed by understanding the cellular mechanisms driving treatment-refractory inflammation and role that this inflammation plays in airway obstruction (4).

Cigarette smoke (CS) is the major cause of airway remodeling by causing cellular injury; injury increases the susceptibility to respiratory pathogens, in particular viruses (5). CS and viruses stimulate similar host danger responses leading to inflammasome activation and enhanced interleukin-1 (IL-1 β) secretion (6-8). Perturbation of IL-1 signaling protects against experimental CS-induced airway remodeling (9, 10). IL-1 β -induced airway remodeling involves increased expression of transforming growth factor- β 1 (TGF- β 1) (11).

TGF- β 1 is a multifunctional cytokine that is widely implicated in both pathologic immunity and fibrosis. However, increased expression of TGF- β is not sufficient for its pathologic effects since it is expressed in latent complex that must be activated in order to function. Binding of the integrin α v β 8 to the latent-TGF- β complex has been shown to be essential for TGF- β activation during development and in driving airway pathology in adult mice (12-20). IL-1 β increases integrin α v β 8 expression and α v β 8-mediated TGF- β activation implicating α v β 8 in CS- and viral-induced airway remodeling (17).

α v β 8 may be involved in the pathogenesis of airway remodeling through its increased COPD-associated expression in airway fibroblasts (17). Intratracheal (IT) adenoviral (Ad) delivery of IL-1 β to the airways of mice causes increased α v β 8 expression, airway inflammation and fibrosis (17). Conditional-deletion of fibroblast α v β 8 prevents Ad-IL-1 β -induced airway inflammation and fibrosis (17).

IL-1 β stimulated primary human or mouse lung fibroblasts become pro-synthetic, increase α v β 8 expression and α v β 8-mediated TGF- β activation and express the potent dendritic cell (DC) chemokine, CCL20 (17). Cytokine arrays of lungs from Ad-IL-1 β -treated mice reveal elevated levels of CCL20 that are reduced by post-natal fibroblast-conditional deletion of *itgb8*, or by treatment with an affinity-matured anti- β 8 antibody, B5 (17, 21). Increased CCL20, DCs and Th₁₇ cells, are associated with airway remodeling induced by CS in combination with the viral mimetic polyinosinic-polycytidylic acid [poly(I:C)], and these increases are efficiently blocked by B5 (21).

CCL20 is increased in COPD lung parenchyma (22); it is the only known chemokine ligand for its receptor, CCR6 (23). Therefore, *ccr6* deficient mice can be used to interrogate the functions of CCL20, *in vivo*. CCR6, which is expressed on immature dendritic cells (DCs), is required for CS-induced DC recruitment and asthma and emphysema phenotypes in mice (23-26). DCs are essential antigen presenting cells implicated in the pathogenesis of COPD through priming pathologic adaptive T-cell immune responses (27). The accumulation of DCs surrounding airways correlate with COPD disease severity (23).

A role for DCs and DC-mediated adaptive T-cell immunity in murine airway remodeling has recently been demonstrated (28). Using *ccr6*-deficient mice, a transgenic diphtheria toxin receptor dendritic cell ablation strategy, or T-cell receptor α -deficient mice, it was determined that *ccr6* expressing DCs and α / β T-cells are required for IL-1 β -mediated airway

inflammation and fibrosis (28). Understanding how and where DCs specifically accumulate in the airways in response to COPD-relevant stimuli may provide biologic insights that can be translated for therapeutic benefit.

Function of DCs in lung disease has largely been inferred from enrichment of specific DC subsets and localization defined by flow cytometry, immunohistochemistry and adoptive transfer of bone-marrow derived DCs (27). Such studies have been instrumental in assigning putative roles and functions to DC subsets in different states of maturation in homeostasis and disease states (29). However, these definitions are based on static information that do not account for dynamic changes that cause DC recruitment and retention in response to endogenous stimuli within complex tissues with physical and geometric constraints (30, 31). Two-photon microscopy allows real-time imaging of immune cells in living tissues where endogenous signals emanate from multiple cell types in distinct microanatomic compartments of the lung. Genetically altered mice expressing fluorescent markers in DCs coupled with 2-photon live cell imaging of living vibratome lung slices allows new insights into DC function (32). Software has also been developed that allows for DCs to be unambiguously identified based on morphologic characteristics (32).

Here we elucidate the dynamic mechanisms, roles and function of DCs in fibroinflammatory airway pathology of COPD by studying mice treated with COPD-relevant stimuli. We report that *ccr6* and the $\alpha\beta$ integrin expressed by fibroblasts regulate DC localization in regions close to the airway lumen by a mechanism involving increased DC chemokinesis.

Materials and Methods

Mice—All mice were bred and housed in specific pathogen-free housing under an IRB approved protocol (IACUC AN098258) and in accordance with the guidelines of the Laboratory Animal Resource Center of the University of California, San Francisco (San Francisco, California). *ccr6* $^{-/-}$ (B6.129P2-*ccr6*^{tm1Dgen}/J), *tcra* $^{-/-}$ (B6.129S2-*tcra*^{tm1Mom}/J), Rosa ^{mT/mG} (B6.129(Cg)-Gt(Rosa)26Sor ^{Tm4(Act-TdTomato,-EGFP)}/J) and WT mice, all in C57BL/6 mice were obtained from The Jackson Laboratory (Bar Harbor, ME). *smad4f/f* mice from Chuxia Deng (National Institutes of Health, NIDDK, Bethesda, MD) were backcrossed 8 generations to C57BL/6. *Colla2-Cre-ER(T)* mice were from Benoit de Crombrugghe (MD Anderson, Houston, TX). Mice expressing human *ITGB8* were generated with a human chromosome BAC (RP11-431K20) containing the entire 80 kb *ITGB8* gene and 70 and 30 kb of 5' and 3' flanking regions (21). Mouse CD11c-EYFP (33) transgenic reporter mice were provided by M. Nussenzweig (The Rockefeller University, New York, NY).

Recombinant Adenovirus—The recombinant E1-E3 deleted type 5 adenovirus, either empty (Ad-C) or expressing human active IL-1 β (Ad-IL-1 β), has been described in detail elsewhere (11). The replication-deficient virus was commercially amplified and purified by cesium chloride gradient centrifugation and PD-10 Sephadex chromatography, plaque titered on 293 cells and checked for wild-type contamination (ViraQuest Inc., North Liberty, IA). Recombinant type 5 Adenoviral vectors expressing Cre-eGFP fusion protein, eGFP, or

LacZ were obtained from the Gene Transfer Vector Core (University of Iowa, Iowa City, IA)

Intratracheal injections—Mice were anesthetized with IP injection of Avertin (250 mg/kg, IP). Then Ad-hIL-1 β or Ad-LacZ (2.5×10^8 pfu in 75 μ l sterile PBS) was instilled intratracheally with a needle (Popper® 24G-1' Straight 1.25mm ball) using the direct visualized instillation (DVI) technique (34). The control was Ad-LacZ.

Cigarette smoke and Polyinosinic:polycytidylic acid (poly I:C) exposure—Mice were exposed using a whole body cigarette smoke (CS) exposure system (Teague Enterprises, CA, USA) within a barrier facility. Mice are acclimated using increasing smoke exposures for 5 days starting at a TSP of 40 mg/m³ for 2 hr, and increasing incrementally to final smoke exposures of 100 TSP using 3R4F cigarettes. Full dose exposures begin in wk 1 with 5 hrs of continuous exposure, with rest on weekends. In week 2, intranasal doses of poly I:C (Invivogen, 50 μ g/dose) are given on days 9 and 12, and again in wk 3 on days 15.

Preparation of lung sections for live cell imaging in the lung—Mice were given a lethal overdose of Avertin and exsanguinated by cutting the renal artery. The lungs and trachea were exposed by cutting through the diaphragm and chest wall. The mice were intubated by tracheotomy with the sheath from an 18-gauge i.v. catheter. Lungs were inflated with 1 ml of 2% low melting temp agarose in sterile PBS maintained at 37°C, and the solution was solidified by briefly rinsing the inflated lungs with PBS at 4°C. Inflated lungs were then excised from the mouse and placed in a sterile 50-ml conical containing RT RPMI without phenol red (Invitrogen, Life Technologies). The left lobe was isolated, cut into 360- μ m sections using a vibratome filled with cool PBS, mounted on plastic slides with Vectabond (3M), and placed in a dish containing RPMI without phenol red before imaging.

Real-time two-photon imaging—A custom resonant-scanning two-photon instrument (32) contains a four-photomultiplier tube detector and collects data at video rate. Where indicated, lung sections were stained with Hoechst for 10 min at a concentration of 100 μ g/ml and then maintained at 36°C in RPMI medium bubbled with 95% O₂ and 5% CO₂ for up to 8 h. The health of lung sections was assessed by ciliary movement in large airways. Samples were excited with a 10-W Mai Tai Ti:Sapphire laser (Spectra-Physics) tuned to a wavelength of 910 nm, and emission wavelengths of 440/40 nm (for Hoechst), 505/20 nm (for GFP), 542/27 nm (for YFP), and 605/70 nm (tdTomato) were collected. Micromanager (Vale Laboratory, UCSF) was used for image acquisition. Each lung section was first surveyed in a raster scan spanning 1567 μ m \times 1300 μ m \times 175 μ m in xyz. For time-lapse acquisition, each xy stack spans 313 μ m \times 260 μ m at a resolution of 0.653 μ m per pixel spaced 3 μ m apart for \sim 100 μ m in z, and 10–20 video-rate frames were averaged.

Imaris-based analysis of motility and morphology—Images were analyzed with Imaris software (Bitplane) using isosurface with masking and spot tracker applications. Three-dimensional images were rendered by Imaris or MetaMorph software (Molecular Devices), and sphericity was calculated by Imaris using the ratio of the surface area of a sphere (with the same volume as the given particle) to the surface area of the particle (32).

Statistical Analysis—All data are reported as means \pm S.E. Comparisons between two different groups were determined using Student's t test for parametric data or Mann-Whitney for non-parametric data. One-way analysis of variance was used for multiple comparisons and Tukey's or Bonferroni's post hoc tests used to test for statistical significance.

Significance was defined as $p < 0.05$. Logistic regression analysis was performed using Stata (v12.1). All other statistical analyses were performed using the software package Prism 4.0b (GraphPad Software, San Diego, CA).

Results

DC accumulate preferentially around small airways in response to IL-1 β

DC function is highly compartmentalized reflecting the distinct antigenic environments of the airways and alveoli (32). We have developed several airway remodeling systems (intratracheal adenoviral IL-1 β , cigarette-smoke (CS) alone, and CS in combination with a viral-mimetic) that we use to directly visualize and quantify live DCs in specific airway compartments to gain fundamental insights into mechanisms of DC antigen surveillance in the airway adjacent zones (17, 21). We used 2-photon microscopy of vibratome living lung slices from mice genetically engineered to express yellow fluorescent protein (YFP) in DCs under control of the mouse CD11c promoter (33). In these mice, YFP bright cells represent both alveolar macrophages (AM) and DCs. Automated image analysis efficiently discriminates between AM and DCs based on sphericity, with the former being "round" and the latter highly complex (32). DCs are preferentially concentrated around airways and alveolar macrophages in the alveolar regions (32).

In response to intratracheal (IT) adenoviral (Ad)-IL-1 β delivery, significantly greater numbers of DCs accumulated around small (<200 μ m) rather than large airways (Fig. 1A-E), which is where DCs accumulate in human COPD, and where the major physiologic site of airway obstruction occurs (35). We therefore focused our subsequent analysis on airways <200 μ m in diameter. Our initial impression was that the number of DCs varied based on the distance from the small airway lumen. To determine where the maximum density of DCs occurred in airway adjacent regions we arbitrarily created four zones, < 25 , 26-50, 51-75, 76-100 and > 100 μ m from the airway lumen (Fig. 1F). The zonal regions that were greater 100 μ m from the airway lumen were defined as the distance to the edge of the image, and generally extended 200-300 μ m from the airway lumen.

DCs accumulate preferentially in a zone located 26-50 μ m from small airways in response to IL-1 β

In Ad-IL-1 β treated WT mice the maximum density of DCs were in a zone 26-50 μ m from the lumen of small airways and the DC density was increased in all zones < 100 μ m compared with the zone > 100 μ m (Fig. 2A, E; Fig. 3A). Ad-IL-1 β also increased numbers of YFP bright cells in the alveolar regions and based on sphericity these were almost all AMs (Fig. 2). We next sought to determine the micro-anatomic distribution of DCs around airways in models that used cigarette smoke (CS), a more physiologically relevant stimulus, to understand how CS influences DC distribution. We used CS alone and in combination with intranasal administration of the viral-mimetic poly (I:C), which synergistically

amplifies CS-induced airway remodeling and mimics the proinflammatory environment that occurs during acute exacerbations of COPD (21). CS or CS plus poly (I:C) caused a similar increase as seen in Ad-IL-1 β treated mice in DC accumulation around airways in all zones < 100 μ m compared with the zone > 100 μ m with a maximal density at 25-50 μ m from the lumen of small airways (Fig. 2I, M; Fig. 3B). These stimuli also increased numbers of YFP bright AMs in the alveolar regions (Fig. 2). To simplify subsequent analyses, we compared zones < 100 μ m between groups of mice.

IL-1 β -induced DC airway accumulation is dependent on *ccr6* and fibroblast expression of *itgb8*

Our recent work has implicated the chemokine CCL20 and its receptor *ccr6* as critical determinants of airway remodeling (17, 21, 28). We therefore investigated the role of *ccr6* in Ad-IL-1 β -induced DC accumulation around murine airways. We found that DC accumulation in all zones within 100 μ m of the airway lumen in *ccr6*-/- mice was significantly reduced (Fig. 2B, F; Fig. 3A). There were no significant differences in DC accumulation in any airway zone between *ccr6*-/- mice treated with Ad-IL-1 β compared to control Ad-LacZ virus (Fig. 3A). Ad-IL-1 β treated WT and *ccr6*-/- mice had similar numbers of AMs (Fig. 2F), consistent with previous reports (28).

IL-1 β -induced DC airway accumulation is dependent on fibroblast expression of *itgb8*

We have previously determined that mouse and human fibroblast expression of the chemokine ligand for *ccr6*, CCL20, is largely dependent on integrin $\alpha v\beta 8$ -mediated TGF- β activation (17). Therefore, we next sought to determine if DC accumulation was dependent on fibroblast expression of $\alpha v\beta 8$. Indeed, DC accumulation around airways was dependent on $\alpha v\beta 8$ expression by fibroblasts since DC accumulation was not seen in Ad-IL-1 β -treated mice with tamoxifen-mediated conditional deletion of *itgb8* selectively on fibroblasts (Fig. 2C, G; Fig. 4A). These effects were not non-specific effects of tamoxifen since Ad-IL-1 β -treated WT mice treated with or without tamoxifen have the same levels of pulmonary inflammation (17). To test if a therapeutic antibody to human $\alpha v\beta 8$ might be useful to inhibit DC accumulation around airways, we treated transgenic (Tg) mice engineered to express human $\beta 8$ (*ITGB8*) with Ad-IL-1 β \pm anti- $\beta 8$, clone B5, as described (21). *ITGB8* Tg mice express $\alpha v\beta 8$ in a similar organ distribution as humans and develop fibrotic airway remodeling in response to Ad-IL-1 β which is blocked by intraperitoneal injection of clone B5 (21). Treatment with B5 efficiently blocked IL-1 β -mediated DC accumulation around airways, and did not have an obvious effect on AM numbers in the alveolar space, consistent with previous reports (Fig. 2D, H; Fig. 4B) (17, 21).

DC airway accumulation in response to cigarette-smoke alone or cigarette-smoke in combination with a viral mimetic is dependent on *ccr6* and fibroblast expression of *itgb8*

To investigate if inhibition of *ccr6*- or $\alpha v\beta 8$ -dependent DC accumulation might block DC accumulation to COPD-relevant stimuli, we used CS-exposure alone, or CS plus poly(I:C) (21). In mice, CS-poly (I:C) exposure causes dramatic DC influx and produces greater airway remodeling than CS exposure alone (21). CS alone significantly increased DC accumulation around airways and CS-poly (I:C) further increased DC accumulation around

airways compared with CS alone (Fig. 3B, 4B). *Ccr6* deficiency (Fig. 2J, N; Fig. 3B), conditional fibroblast deletion of *itgb8* (Fig. 2K, O; Fig. 4C), or B5 treatment of *ITGB8* Tg mice (Fig. 2L, P; Fig. 4D), resulted in significantly decreased DC accumulation around airways in response to CS alone or CS plus poly(I:C). These treatments had little effect on AM accumulation in the alveolar parenchyma, consistent with previous reports (21, 28). The nearly identical findings with genetic deletion of β 8 on fibroblasts, β 8 antibody inhibition, or *ccr6* deficiency in Ad-IL-1 β -, CS-, or CS plus poly(I:C)-treated mice support the hypothesis that $\alpha\beta$ 8-mediated activation of TGF- β by fibroblasts is crucial for CCL20 expression and *ccr6*-dependent DC recruitment during airway remodeling.

***ccr6* and fibroblast expression of *itgb8* are required for IL-1 β induced DC chemokinesis**

DC localization around airways can conceptually be due to increased influx from the circulation or a redistribution of DCs from airway-distal towards airway-adjacent regions. The former would be driven primarily by increased motility (chemokinesis) and the latter by directed migration (chemotaxis). Automated image analysis of vibratome lung slices from Ad-IL-1 β treated mice revealed significantly increased DC velocity in all zones located within 100 μ m from the airway lumen compared to airway distal zones greater than 100 μ m (Fig. 5A). Increased IL-1 β -dependent DC velocity in the zone within 100 μ m from the airway was dependent on CCL20 expression since it was not seen in *ccr6* -/- mice (Fig. 5A). DC velocity was similarly increased by CS-exposure in zones within 50 μ m from the airway lumen and was also dependent on *ccr6* expression (Fig. 5B). There was general increase in DC velocity in the airway adjacent zones (<100 μ m from the airway lumen) compared to the airway distal regions (>100 μ m) in all groups except WT control (Ad-LacZ or room air) mice (Fig. 5A, B). Ad-IL-1 β -, CS- or CS-poly (I:C)-induced chemokinesis was dependent on $\alpha\beta$ 8 expression specifically on fibroblasts since BAC *ITGB8* Tg mice treated with B5 had significantly decreased DC chemokinesis in airway adjacent zones <100 μ m (Fig. 6A), as did mice with fibroblast-specific deletion of β 8 (Fig. 6B), or treated with anti- β 8, clone B5 (Fig. 6C)

To determine the role of chemotaxis in DC accumulation around airways, the directional non-random migration of individual DCs located within 100 μ m of the airway lumen was determined. To measure directional migration, mean-square displacement (MSD) over time was calculated. Cells in a chemotactic gradient follow a non-random pattern of movement and MSD will increase non-linearly with time (36, 37). We established a time course of velocity and directionality of airway DCs within 100 μ m of the airway lumen after Ad-IL- β treatment to determine if DC behavior changes over the experimental period as the airways become progressively inflamed, DCs are recruited and differentiate (Fig 6D). We have previously determined that elevated lung DC numbers appear on day 5 and persist through day 9 following Ad-IL- β treatment (28). Therefore, we studied velocity and migration at days 5 and 9 following Ad-IL- β treatment compared to controls (Ad-LacZ). MSD vs. time of DCs from mice at day 5 and 9 post-treatment with Ad-IL-1 β or day 5 post-treatment with Ad-LacZ were near perfect fits ($r^2=0.98, 0.97, 0.96$, respectively) to a linear regression model (Fig. 6D). Linearity indicates random movement and not biased directionality (i.e. chemotaxis). The slopes [a.k.a. migration coefficient (38)], which positively correlate with migratory velocity, were significantly increased by Ad-IL-1 β - compared with Ad-LacZ at

both days 5 and 9 post-treatment (Fig. 6D). There was not a significant difference in DC migration coefficient between mice at days 5 and 9 post- Ad-IL-1 β treatment (Fig. 6D).

We compared MSD over time in Ad-IL-1 β -, CS- or CS-poly(I:C)-treated mice. MSD over time in all groups of mice was essentially linear and the slope nearly equal in Ad-IL-1 β -, CS- or CS-poly(I:C)-treated mice, consistent with similar random non-directional migration (Fig. 6E, $r^2=0.9893, 0.9418, 0.9932$, respectively). The MSD remained linear and the slopes were nearly equal in Ad-IL-1 β -, CS- or CS plus poly I:C-treated mice deficient in *ccr6*, with conditional deletion of $\beta 8$ on fibroblasts, or BAC *ITGB8* mice treated with B5 (Fig. 6E). The migration coefficients were significantly decreased in the groups deficient in *ccr6*, with fibroblast conditional deletion of *itgb8*, or BAC *ITGB8* Tg mice treated with B5 (Fig. 6E). Taken together, these results demonstrate that chemokinesis, not chemotaxis drive increased DC accumulation around airways; *ccr6*-dependent DC chemokinesis requires fibroblast *itgb8* expression.

Discussion

This study has advanced the mechanistic understanding of dendritic cell accumulation around murine airways in response to COPD-relevant stimuli. We have defined the functional effects of $\alpha\beta 8$ and *ccr6* on DC migratory behavior by demonstrating that DC chemokinesis rather than chemotaxis is the primary mechanism leading to DC accumulation around airways.

Dynamic imaging of live lung DCs reveal novel insights into DC behavior, in vivo—2-photon imaging of living lung tissue allowed us to address the microanatomic localization and movement of DCs in relation to their migratory velocity and directionality. We gained the following novel insights into DC behavior using both Ad-IL-1 β and CS- and CS-poly (I:C) models: 1) DCs preferentially accumulate around small rather than large airways, 2) DCs accumulate preferentially in a zone 26-50 μ m from the airway lumen, in close proximity to airway fibroblasts and airway epithelium, the important CCL20 expressing cell types (22), 3) DCs in airway adjacent zones show marked increases in chemokinetic behavior, but do not show bulk directional movement towards or away from airways, 4) alveolar DCs show relatively very little movement and do not preferentially move toward airways, 5) airway DCs show similar migratory behavior in response to diverse pro-inflammatory stimuli.

The preferential accumulation of DCs around the small airways in response to Ad-IL-1 β , CS, or CS + poly I:C likely reflects increased exposure to these stimuli; the surface area of the small airways account for over 20% of the lung volume compared with the large airways which account for $\sim 2\%$ (39). The similarity of behavior of DCs in specific airway adjacent zones in response to a variety of stimuli likely implies dominant underlying signaling mechanisms and anatomic and geometric specialization of the airway adjacent zones of small airways to facilitate antigen surveillance by DCs. We have determined that activity of IL-1 β , TGF- β (via increased $\alpha\beta 8$ -mediated activation of TGF- β) and ccl20/ccr6 are increased in Ad-IL1 β , CS or CS +poly I:C stimulated mice (17, 21), which conspires to increase DC chemokinesis. Overall, these data suggest that the bulk of airway DC

Author Manuscript

Author Manuscript

Author Manuscript

Author Manuscript

populations are functionally homogeneous in chemotactic and chemokinetic behavior in response to diverse proinflammatory stimuli, originate from a non-alveolar compartment, and differ from the alveolar DC population in migratory behavior.

ccr6- and fibroblast $\alpha\beta8$ -dependent DC chemokinesis—DC chemokinesis is critically dependent on *ccr6*, and fibroblast expression of $\alpha\beta8$. In Ad-IL-1 β and/or CS-treated mice with *ccr6*-deficiency, fibroblast *itgb8*-deficiency, or global antibody inhibition of $\alpha\beta8$, DCs did not accumulate around airways or show significant increases in velocity. These data complement recent data demonstrating that fibroblast $\alpha\beta8$ -mediated TGF- β activation is essential for enhancing fibroblast secretion of CCL20 around airways (22). These observations suggest that the $\alpha\beta8/CCL20/IL-1\beta$ axis is required for increased DC influx close to the airway in response to pathologic stimuli. Indeed, we have recently determined that $\alpha\beta8$, CCL20 and IL-1 β , are increased in COPD lung parenchyma compared to smokers without COPD and/or non-smoking controls; both $\alpha\beta8$ and IL-1 β expression levels are significantly correlated with CCL20 levels (22).

The mechanisms underlying the difference in migratory behavior between airway and alveolar DCs may be due to differences in CCR6 expression by DCs localized in these respective compartments. However, the enhanced velocity of DCs within the zone 26-50 μm of the airway lumen suggests that airway-centric CCL20 expression gradients might be a more plausible explanation. Such a CCL20-gradient might be established by the fibroblasts closest to the airway lumen, which have the greatest exposure to signals emanating from airway epithelial cells, such as IL-1 β (17). Indeed, CCL20 immunostaining is increased in airway fibroblasts and epithelium in COPD lung samples (22).

Other chemokines are also released by epithelial cells and fibroblasts that could positively or negatively influence DC velocity close to the airway lumen. Our data reveal the importance of other such chemokines since *ccr6*-deficient DCs in steady-state conditions (i.e. with Ad-LacZ) displayed a higher baseline migratory velocity than WT-DCs. The differences in baseline migration were seen within 25 μm of the airway lumen suggesting the importance of signals emanating from airway epithelial cells or the underlying mesenchymal cells. The identity of these compensatory chemokines/chemokine receptors that are likely upregulated in *ccr6*-deficient mice were not investigated in this present study since they did not appear to influence DC velocity under proinflammatory conditions. Our previous work would suggest that CCL2 is a likely candidate since it is abundantly expressed by airway cell types and its receptor CCR2 is expressed by DCs (17).

How do DCs accumulate around airways and where do they come from?

Airway DCs are terminally differentiated and have a half-life between 1 and 2 days (40). As such, after Ad-IL-1 β treatment, an incoming source of DCs must be accessed to maintain high DC numbers around the airways. Increased DCs numbers around airways might occur by a number of mechanisms, alone or in combination: 1) increased chemokinesis, 2) increased local retention, or 3) decreased emigration (Fig. 7). The first possibility would be manifested by increased overall flow of DCs with balanced immigration and emigration; the second and third, by decreased mean velocity and biased directionality. Our results suggest that increased chemokinesis and not chemotaxis is the major driving force leading to DC

accumulation around airways. The predicted biologic consequence of increased random DC movement would be corresponding increases in the chance of antigen encounter, interaction with lymphatics and emigration to the draining lymph node, which would stimulate adaptive immune responses. Indeed, in the Ad-IL-1 β model we have found evidence of a dramatic increase in lung DCs migrating to the draining lymph node, which corresponds with an increase in adaptive CD4+ T-cell numbers (17). Finally, our data do not support the existence of specific DC chemotactic or retention signals around airways, but we cannot exclude the existence of such signals which influence the chemotaxis of minor subsets of DCs which might not be detected our cell tracking software.

Two main subsets of classical airway DCs have been described that are increased in the Ad-IL-1 β model, the most numerous (>90% of lung DCs) located in the interstitium of the airway wall and a relatively rare population intermingled with the airway epithelium (<10% of lung DCs). The former express CD11b but not CD103 (CD11b+ DCs) and the latter do not express CD11b but express CD103 (CD103+ DCs) (17, 27). In response to Ad-IL-1 β , CS, CS-poly(I:C), RSV or aspergillus, *ccr6*-dependent increases in DC number are predominantly seen in the CD11b+ subset (17, 41, 42). The main *ccr6* expressing immune cell population that increases in number in the Ad-IL-1 β model is the CD11b + DC subset (28). In response to Ad-IL-1 β or influenza infection, murine CD11b+ DCs migrate efficiently to the draining mediastinal lymph node (MLN) and the kinetics of CD11b+ DCs in lung and later in the MLN correlates with adaptive T-cell responses indicating the importance of DCs in T-cell priming (17, 43). Thus, these previous studies along with the anatomic location of DCs around airways suggest that here we are mainly detecting the movement of the CD11b+ DC subset.

The possible origins of airway CD11b+ DCs remains somewhat controversial, either differentiating from a monocyte or a pre-DC precursor (44). In the Ad-IL-1 β and influenza models, most of the CD11b+ DCs express intermediate levels of Ly6c suggesting a monocytic lineage (17, 28, 43). No previous studies have addressed how or if CD11b+ DCs localize specifically to the airways in response to COPD-relevant proinflammatory stimuli. Our data reinforce the evidence that CD11b+ DCs are the main airway DC subset, are monocyte derived, arrive by a hematogenous route and do not redistribute from the alveoli.

Implications of increased DC accumulation and chemokinesis—One of the major putative mechanisms of chronic inflammation causing airway obstruction is through airway narrowing due to cicatricial airway fibrosis (35). How, or if, immune responses contribute to the development of fibrosis remains controversial. The temporal relationship between CD11b⁺ DC accumulation, adaptive Th₁₇ immunity and airway fibrosis suggest that DCs are important proximal cell types in the fibroinflammatory response (21, 23, 28, 35). We have recently determined that *ccr6* deficiency or DC depletion protects against experimental airway fibrosis (28). Increased integrin $\alpha\gamma\beta\delta$ -dependent expression of the DC chemokine CCL20, from airway fibroblasts may be critical in this pathogenic sequence (17, 21, 22). Therefore, our observations provide a basis for the hypotheses that increased *ccr6*/ccl20-dependent DC chemokinesis is involved in airway remodeling.

Targeting DC chemokinesis in COPD?—Data obtained in mouse models may be relevant to human COPD, but there are a number of caveats that must be considered. A general feature of human COPD is that the fibroinflammatory process is progressive, even following smoking cessation, while in mouse models fibrosis is transient, and resolution begins when the stimulus is removed (11, 45-47). This likely reflects the short transient exposures required to accommodate the relatively short life span of mice, but may also reflect fundamental anatomic and biologic differences between mice and human (48). Definitive demonstration of the relevance of our findings in mice to human lung DC trafficking remains to be shown.

Because of the central role that DCs play in innate and adaptive immunity, broadly targeting DC function in humans should be approached with caution. Selective inhibition of DC chemokinesis might temper the adaptive immune response and reduce the chronic inflammation in the airways of COPD patients. Such a selective perturbation of DC motion would temper the risk of global inhibition of DC function or DC ablation. Here, we confirm that inhibiting $\alpha v\beta 8$ -mediated activation of TGF- β in mice blocks central pathways required for DC chemokinesis, in particular those dependent on the ccr6/CCL20 axis.

We have recently found that $\alpha v\beta 8$ -mediated activation of TGF- β induces a SMAD4-NF κ B transcription complex on the human CCL20 promoter, which enhances CCL20 transcription (22). Both $\alpha v\beta 8$ and CCL20 are increased in the parenchyma of human COPD patients, and their expression is significantly correlated (22). Inhibition of $\alpha v\beta 8$ -mediated TGF- β activation provides additional potential effects of blocking the expression of TGF- β -dependent collagen production as well as other cytokines (i.e. IL-1 β (17)), chemokines (i.e. CCL2 and CCL7 (17)), expressed by the structural airway cell types where $\alpha v\beta 8$ is expressed (fibroblasts and airway epithelial cells)(4, 49).

The enhanced expression of $\alpha v\beta 8$ in COPD, the cell-type specificity, and the demonstrated efficacy of inhibiting $\alpha v\beta 8$ -mediated TGF- β activation in prevention of experimental airway remodeling (21), together with the mechanistic insights provided here, suggest that $\alpha v\beta 8$ - and/or CCR6/CCL20-dependent DC chemokinesis could play a role in the evolution of chronic airway disease in COPD.

Acknowledgments

We thank M. Nussenzweig for CD11c-EYFP mice and Benoit de Crombrugghe for Col1a2-Cre-ER(T) mice.

Footnotes: This work was supported by the grants from the NIH HL113032, HL063993, HL090662, NS044155, UCTRDRP, UCSF Academic Senate, UCOP POC award (S.L.N.), UCSF Liver Center (P30DK026743) to (S.L.N. and J.L.B.).

References

1. Miniño AM, Xu JQ, Kochanek KD. Deaths: Preliminary data for 2008. National Vital Statistics Reports. 2010;59.
2. Ito K, Ito M, Elliott WM, Cosio B, Caramori G, Kon OM, Barczyk A, Hayashi S, Adcock IM, Hogg JC, Barnes PJ. Decreased histone deacetylase activity in chronic obstructive pulmonary disease. *N Engl J Med.* 2005; 352:1967–1976. [PubMed: 15888697]

3. Postma DS, Timens W. Remodeling in asthma and chronic obstructive pulmonary disease. *Proc Am Thorac Soc*. 2006; 3:434–439. [PubMed: 16799088]
4. Araya J, Cambier S, Markovics JA, Wolters P, Jablons D, Hill A, Finkbeiner W, Jones K, Broaddus VC, Sheppard D, Barczak A, Xiao Y, Erle DJ, Nishimura SL. Squamous metaplasia amplifies pathologic epithelial-mesenchymal interactions in copd patients. *J Clin Invest*. 2007; 117:3551–3562. [PubMed: 17965775]
5. Papi A, Bellettato CM, Braccioni F, Romagnoli M, Casolari P, Caramori G, Fabbri LM, Johnston SL. Infections and airway inflammation in chronic obstructive pulmonary disease severe exacerbations. *Am J Respir Crit Care Med*. 2006; 173:1114–1121. [PubMed: 16484677]
6. Lucattelli M, Cicko S, Muller T, Lommatsch M, De Cunto G, Cardini S, Sundas W, Grimm M, Zeiser R, Durk T, Zissel G, Sorichter S, Ferrari D, Di Virgilio F, Virchow JC, Lungarella G, Idzko M. P2 \times 7 receptor signaling in the pathogenesis of smoke-induced lung inflammation and emphysema. *Am J Respir Cell Mol Biol*. 2011; 44:423–429. [PubMed: 20508069]
7. Geraghty P, Dabo AJ, D'Armiento J. Tlr4 protein contributes to cigarette smoke-induced matrix metalloproteinase-1 (mmp-1) expression in chronic obstructive pulmonary disease. *J Biol Chem*. 2011; 286:30211–30218. [PubMed: 21730072]
8. Kang MJ, Lee CG, Lee JY, Dela Cruz CS, Chen ZJ, Enelow R, Elias JA. Cigarette smoke selectively enhances viral pamp- and virus-induced pulmonary innate immune and remodeling responses in mice. *J Clin Invest*. 2008; 118:2771–2784. [PubMed: 18654661]
9. Churg A, Zhou S, Wang X, Wang R, Wright JL. The role of interleukin-1 β in murine cigarette smoke-induced emphysema and small airway remodeling. *Am J Respir Cell Mol Biol*. 2009; 40:482–490. [PubMed: 18931327]
10. Doz E, Noulin N, Boichot E, Guenon I, Fick L, Le Bert M, Lagente V, Ryffel B, Schnyder B, Quesniaux VF, Couillin I. Cigarette smoke-induced pulmonary inflammation is tlr4/myd88 and il-1r1/myd88 signaling dependent. *J Immunol*. 2008; 180:1169–1178. [PubMed: 18178857]
11. Kolb M, Margetts PJ, Anthony DC, Pitossi F, Gauldie J. Transient expression of il-1 β induces acute lung injury and chronic repair leading to pulmonary fibrosis. *J Clin Invest*. 2001; 107:1529–1536. [PubMed: 11413160]
12. Mu D, Cambier S, Fjellbirkeland L, Baron JL, Munger JS, Kawakatsu H, Sheppard D, Broaddus VC, Nishimura SL. The integrin alpha(v)beta8 mediates epithelial homeostasis through mt1-mmp-dependent activation of tgf-beta1. *J Cell Biol*. 2002; 157:493–507. [PubMed: 11970960]
13. Munger JS, Harpel JG, Giancotti FG, Rifkin DB. Interactions between growth factors and integrins: Latent forms of transforming growth factor-beta are ligands for the integrin alphavbeta1. *Mol Biol Cell*. 1998; 9:2627–2638. [PubMed: 9725916]
14. Wipff PJ, Rifkin DB, Meister JJ, Hinz B. Myofibroblast contraction activates latent tgf-beta1 from the extracellular matrix. *J Cell Biol*. 2007; 179:1311–1323. [PubMed: 18086923]
15. Munger JS, Huang X, Kawakatsu H, Griffiths MJ, Dalton SL, Wu J, Pittet JF, Kaminski N, Garat C, Matthay MA, Rifkin DB, Sheppard D. The integrin alpha v beta 6 binds and activates latent tgf beta 1: A mechanism for regulating pulmonary inflammation and fibrosis. *Cell*. 1999; 96:319–328. [PubMed: 10025398]
16. Aluwhare P, Mu Z, Zhao Z, Yu D, Weinreb PH, Horan GS, Violette SM, Munger JS. Mice that lack activity of alphavbeta6- and alphavbeta8-integrins reproduce the abnormalities of tgf β 1- and tgf β 3-null mice. *J Cell Sci*. 2009; 122:227–232. [PubMed: 19118215]
17. Kitamura H, Cambier S, Somanath S, Barker T, Minagawa S, Markovics J, Goodsell A, Publicover J, Reichardt L, Jablons D, Wolters P, Hill A, Marks JD, Lou J, Pittet JF, Gauldie J, Baron JL, Nishimura SL. Mouse and human lung fibroblasts regulate dendritic cell trafficking, airway inflammation, and fibrosis through integrin alphavbeta8-mediated activation of tgf-beta. *J Clin Invest*. 2011; 121:2863–2875. [PubMed: 21646718]
18. Kudo M, Melton AC, Chen C, Engler MB, Huang KE, Ren X, Wang Y, Bernstein X, Li JT, Atabay K, Huang X, Sheppard D. Il-17a produced by alphabeta t cells drives airway hyper-responsiveness in mice and enhances mouse and human airway smooth muscle contraction. *Nat Med*. 2012; 18:547–554. [PubMed: 22388091]
19. Melton AC, Bailey-Bucktrout SL, Travis MA, Fife BT, Bluestone JA, Sheppard D. Expression of alphavbeta8 integrin on dendritic cells regulates th17 cell development and experimental

autoimmune encephalomyelitis in mice. *J Clin Invest.* 2010; 120:4436–4444. [PubMed: 21099117]

20. Travis MA, Reizis B, Melton AC, Masteller E, Tang Q, Proctor JM, Wang Y, Bernstein X, Huang X, Reichardt LF, Bluestone JA, Sheppard D. Loss of integrin alpha(v)beta8 on dendritic cells causes autoimmunity and colitis in mice. *Nature.* 2007; 449:361–365. [PubMed: 17694047]

21. Minagawa S, Lou J, Seed RI, Cormier A, Wu S, Cheng Y, Murray L, Tsui P, Connor J, Herbst R, Govaerts C, Barker T, Cambier S, Yanagisawa H, Goodsell A, Hashimoto M, Brand OJ, Cheng R, Ma R, McKnelly KJ, Wen W, Hill A, Jablons D, Wolters P, Kitamura H, Araya J, Barczak AJ, Erle DJ, Reichardt LF, Marks JD, Baron JL, Nishimura SL. Selective targeting of tgf-beta activation to treat fibroinflammatory airway disease. *Science translational medicine.* 2014; 6:241ra279.

22. Brand OJ, Somanath S, Moermans C, Yanagisawa H, Hashimoto M, Cambier S, Markovics J, Bondesson AJ, Hill A, Jablons D, Wolters P, Lou J, Marks JD, Baron JL, Nishimura SL. Transforming growth factor-beta and interleukin-1beta signaling pathways converge on the chemokine ccl20 promoter. *J Biol Chem.* 2015 Press.

23. Demedts IK, Bracke KR, Van Pottelberge G, Testelmans D, Verleden GM, Vermassen FE, Joos GF, Brusselle GG. Accumulation of dendritic cells and increased ccl20 levels in the airways of patients with chronic obstructive pulmonary disease. *Am J Respir Crit Care Med.* 2007; 175:998–1005. [PubMed: 17332482]

24. Bracke KR, D'Hulst AI, Maes T, Moerloose KB, Demedts IK, Lebecque S, Joos GF, Brusselle GG. Cigarette smoke-induced pulmonary inflammation and emphysema are attenuated in ccr6-deficient mice. *J Immunol.* 2006; 177:4350–4359. [PubMed: 16982869]

25. Aubert JD, Dalal BI, Bai TR, Roberts CR, Hayashi S, Hogg JC. Transforming growth factor beta 1 gene expression in human airways. *Thorax.* 1994; 49:225–232. [PubMed: 8202878]

26. Schroder K, Zhou R, Tschopp J. The nlrp3 inflammasome: A sensor for metabolic danger? *Science.* 2010; 327:296–300. [PubMed: 20075245]

27. Lambrecht BN, Hammad H. Biology of lung dendritic cells at the origin of asthma. *Immunity.* 2009; 31:412–424. [PubMed: 19766084]

28. Hashimoto M, Yanagisawa H, Minagawa S, Sen D, Goodsell A, Ma R, Moermans C, McKnelly KJ, Baron JL, Krummel MF, Nishimura SL. A critical role for dendritic cells in the evolution of il-1beta-mediated murine airway disease. *J Immunol.* 2015; 194:3962–3969. [PubMed: 25786688]

29. Zhang N, Bevan MJ. Tgf-beta signaling to t cells inhibits autoimmunity during lymphopenia-driven proliferation. *Nat Immunol.* 2012; 13:667–673. [PubMed: 22634866]

30. Vignola AM, Chanze P, Chiappara G, Merendino A, Pace E, Rizzo A, la Rocca AM, Bellia V, Bonsignore G, Bousquet J. Transforming growth factor-beta expression in mucosal biopsies in asthma and chronic bronchitis. *Am J Respir Crit Care Med.* 1997; 156:591–599. [PubMed: 9279245]

31. Border WA, Noble NA. Transforming growth factor beta in tissue fibrosis. *N Engl J Med.* 1994; 331:1286–1292. [PubMed: 7935686]

32. Thornton EE, Looney MR, Bose O, Sen D, Sheppard D, Locksley R, Huang X, Krummel MF. Spatiotemporally separated antigen uptake by alveolar dendritic cells and airway presentation to t cells in the lung. *The Journal of experimental medicine.* 2012; 209:1183–1199. [PubMed: 22585735]

33. Lindquist RL, Shakhar G, Dudziak D, Wardemann H, Eisenreich T, Dustin ML, Nussenzweig MC. Visualizing dendritic cell networks in vivo. *Nat Immunol.* 2004; 5:1243–1250. [PubMed: 15543150]

34. Ganter MT, Roux J, Miyazawa B, Howard M, Frank JA, Su G, Sheppard D, Violette SM, Weinreb PH, Horan GS, Matthay MA, Pittet JF. Interleukin-1beta causes acute lung injury via alphavbeta5 and alphavbeta6 integrin-dependent mechanisms. *Circ Res.* 2008; 102:804–812. [PubMed: 18276918]

35. Hogg JC, Chu F, Utokaparch S, Woods R, Elliott WM, Buzatu L, Cherniack RM, Rogers RM, Sciurba FC, Coxson HO, Pare PD. The nature of small-airway obstruction in chronic obstructive pulmonary disease. *N Engl J Med.* 2004; 350:2645–2653. [PubMed: 15215480]

36. Saxton MJ. Single-particle tracking: The distribution of diffusion coefficients. *Biophysical journal*. 1997; 72:1744–1753. [PubMed: 9083678]
37. Saxton MJ, Jacobson K. Single-particle tracking: Applications to membrane dynamics. *Annual review of biophysics and biomolecular structure*. 1997; 26:373–399.
38. Miller MJ, Wei SH, Parker I, Cahalan MD. Two-photon imaging of lymphocyte motility and antigen response in intact lymph node. *Science*. 2002; 296:1869–1873. [PubMed: 12016203]
39. Thurlbeck, WM.; Churg, A. *Thurlbeck's pathology of the lung*. New York: Thieme; 2005.
40. Holt PG, Haining S, Nelson DJ, Sedgwick JD. Origin and steady-state turnover of class ii mhc-bearing dendritic cells in the epithelium of the conducting airways. *J Immunol*. 1994; 153:256–261. [PubMed: 8207240]
41. Kallal LE, Schaller MA, Lindell DM, Lira SA, Lukacs NW. Ccl20/CCR6 blockade enhances immunity to rsv by impairing recruitment of dc. *Eur J Immunol*. 2010; 40:1042–1052. [PubMed: 20101616]
42. Phadke AP, Akangire G, Park SJ, Lira SA, Mehrad B. The role of CC chemokine receptor 6 in host defense in a model of invasive pulmonary aspergillosis. *Am J Respir Crit Care Med*. 2007; 175:1165–1172. [PubMed: 17379855]
43. Ballesteros-Tato A, Leon B, Lund FE, Randall TD. Temporal changes in dendritic cell subsets, cross-priming and costimulation via CD70 control CD8(+) T cell responses to influenza. *Nat Immunol*. 2010; 11:216–224. [PubMed: 20098442]
44. Lambrecht BN, Hammad H. Lung dendritic cells in respiratory viral infection and asthma: From protection to immunopathology. *Annual review of immunology*. 2012; 30:243–270.
45. Kisseeleva T, Cong M, Paik Y, Scholten D, Jiang C, Benner C, Iwaisako K, Moore-Morris T, Scott B, Tsukamoto H, Evans SM, Dillmann W, Glass CK, Brenner DA. Myofibroblasts revert to an inactive phenotype during regression of liver fibrosis. *Proc Natl Acad Sci U S A*. 2012; 109:9448–9453. [PubMed: 22566629]
46. Moeller A, Ask K, Warburton D, Gauldie J, Kolb M. The bleomycin animal model: A useful tool to investigate treatment options for idiopathic pulmonary fibrosis? *The international journal of biochemistry & cell biology*. 2008; 40:362–382. [PubMed: 17936056]
47. Araya J, Nishimura SL. Fibrogenic reactions in lung disease. *Annu Rev Pathol*. 2010; 5:77–98. [PubMed: 20078216]
48. Irvin CG, Bates JH. Measuring the lung function in the mouse: The challenge of size. *Respiratory research*. 2003; 4:4. [PubMed: 12783622]
49. Araya J, Cambier S, Morris A, Finkbeiner W, Nishimura SL. Integrin-mediated transforming growth factor-beta activation regulates homeostasis of the pulmonary epithelial-mesenchymal trophic unit. *Am J Pathol*. 2006; 169:405–415. [PubMed: 16877343]
50. Zheng B, Zhang Z, Black CM, de Crombrugge B, Denton CP. Ligand-dependent genetic recombination in fibroblasts: A potentially powerful technique for investigating gene function in fibrosis. *Am J Pathol*. 2002; 160:1609–1617. [PubMed: 12000713]

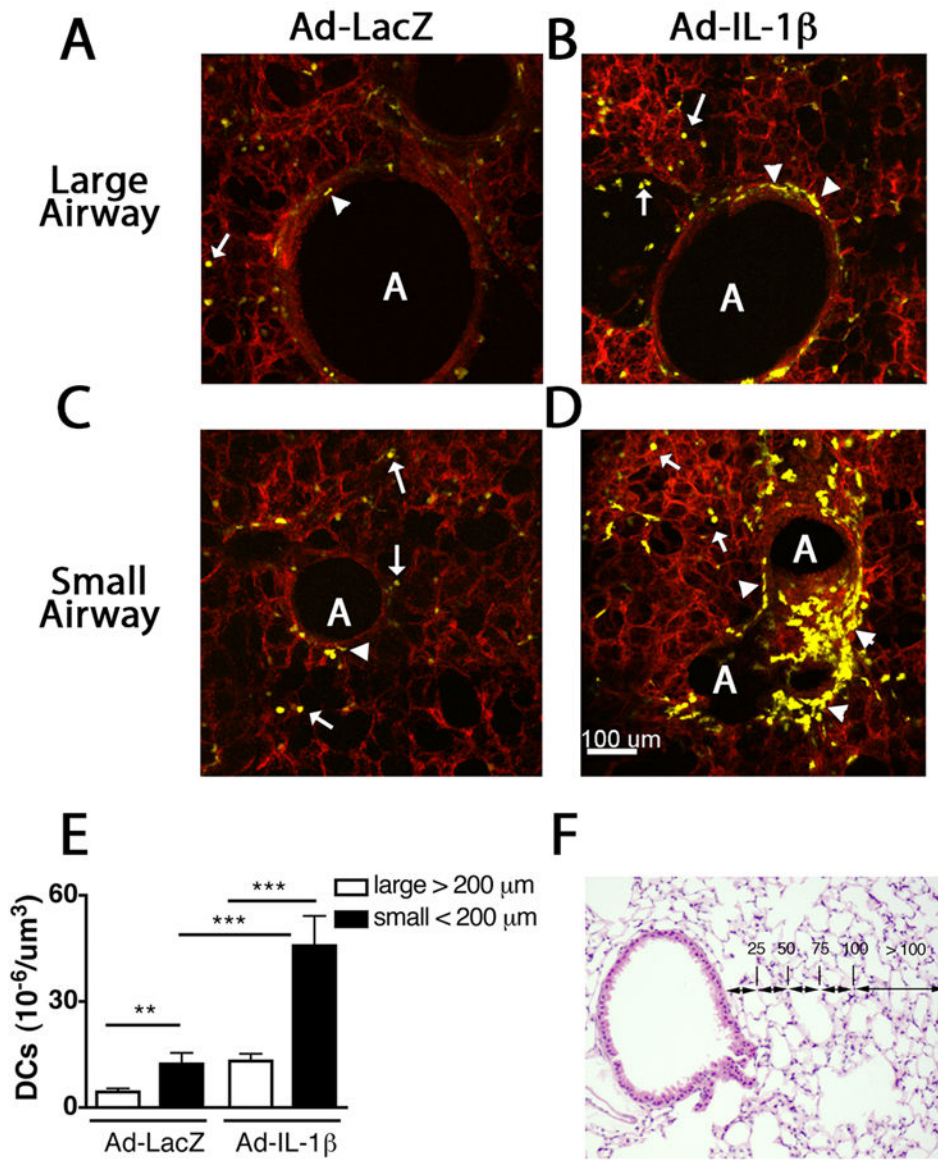


Fig. 1. DCs primarily localize around small airways in mice treated with intratracheal Ad-IL-1 β
 CD11c-YFP mice were treated either with Ad-LacZ (A, C) or Ad-IL-1 β (B, D).

Representative static Z-stack images from 2-photon microscopy of living vibratome lung sections of transgenic mice (Tg) expressing YFP under control of the CD11c promoter (in DCs and alveolar macrophages) 9 days after infection. Large (>200 μ m) and small (<200 μ m in lumen diameter) airways are shown in A, B or C, D, respectively. E) Image analysis (Imaris, Bitplane, Zurich, Switzerland) reveals significantly more DCs around small compared to large airways (A) in both steady state (Ad-LacZ) controls and Ad-IL-1 β -treated mice. DCs (arrowheads) have complex cell contours and are located close to the airways and round AMs (arrows) are located mainly in the alveolar parenchyma. N=3 in control and N 5 in Ad-IL-1 β -treated groups from three independent experiments. F) Schematic of airway adjacent zones used to assess microanatomic localization of DCs. **p<0.01, ***p<0.001

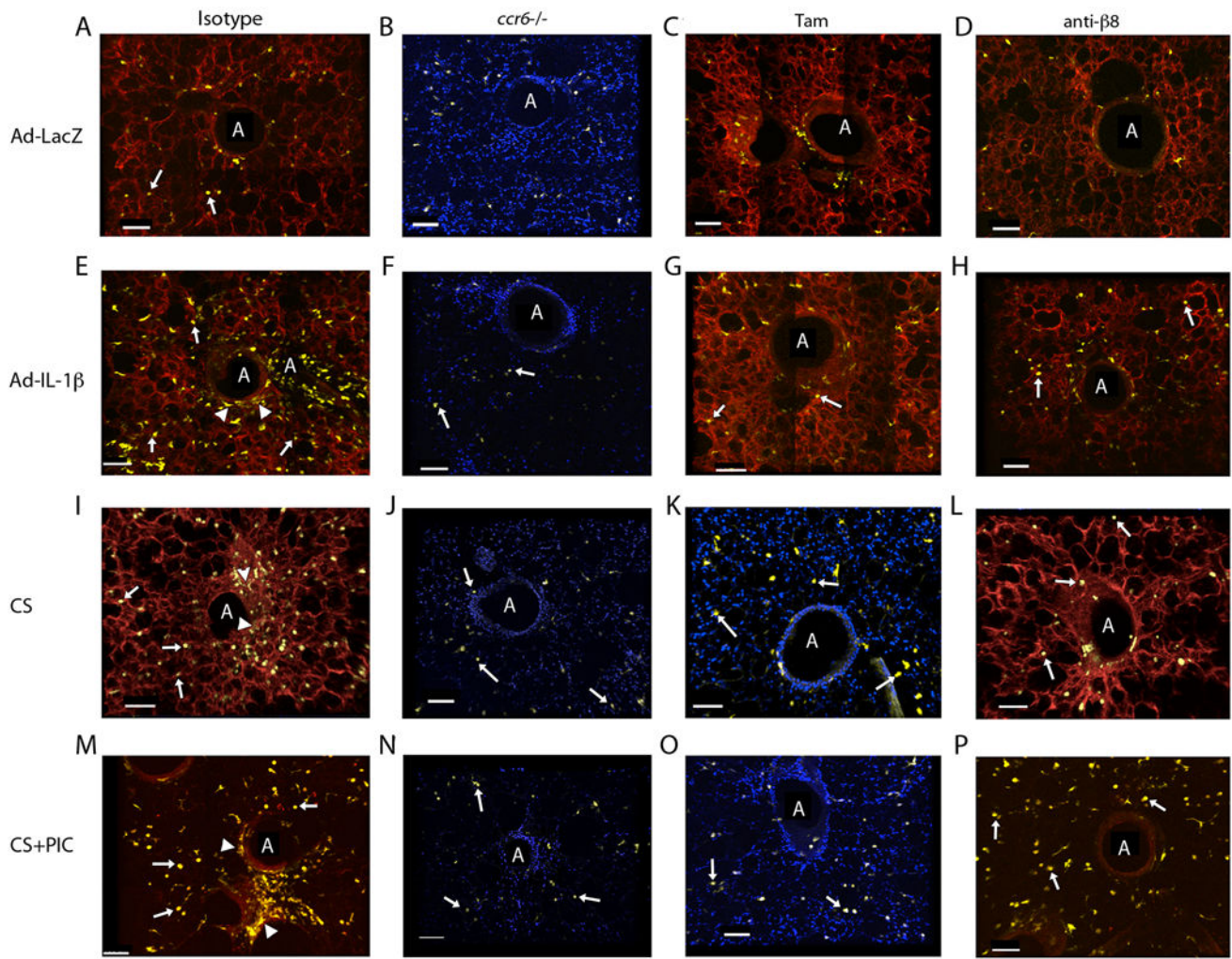


Fig. 2. *ccr6* expression by DCs and *itgb8* expression by fibroblasts mediate DC accumulation around airways in Ad-IL-1 β -and cigarette smoke (CS)-treated mice

Representative static Z-stack images from 2-photon microscopy of living vibratome lung sections of transgenic mice (Tg) expressing YFP under control of the CD11c promoter (in DCs and alveolar macrophages). CD11c-YFP mice were crossed to either WT, BAC *ITGB8* Tg; *itgb8*-/- (A, D, E, H, I, L, M, P), col-cre-ER(T); *ccr6* -/- (B, F, J, N) or *itgb8f/f* (C, G, K, O). Mice were treated either with Ad-LacZ (A-D); Ad-IL-1 β (E-H); CS (I-L); CS-poly(I:C)(PIC) (M-P); isotype control antibody (A, E, I, M), tamoxifen (Tam, C, G, K, O), or anti- β 8, clone B5 (B, F, J, N). Bar=100 μ m. A=Airway lumen. DCs (arrowheads) have complex cell contours and are located close to the airways and round AMs (arrows) are located mainly in the alveolar parenchyma. Lung sections were harvested from mice 9 days after Ad-LacZ or Ad-IL-1 β 16 days after the initiation of smoke exposure, or 16 days after the initiation of the combined CS and PIC protocol. $N=3$ for control groups and at least 6 from Ad-IL-1 β -treated groups from at least three independent experiments. Composite photomicrographs were created with IMARIS. Blue background represents counterstained sections with Hoechst. Red background represents mice crossed to transgenic mice expressing a membrane Tomato (mT) under the ubiquitous Rosa promoter.

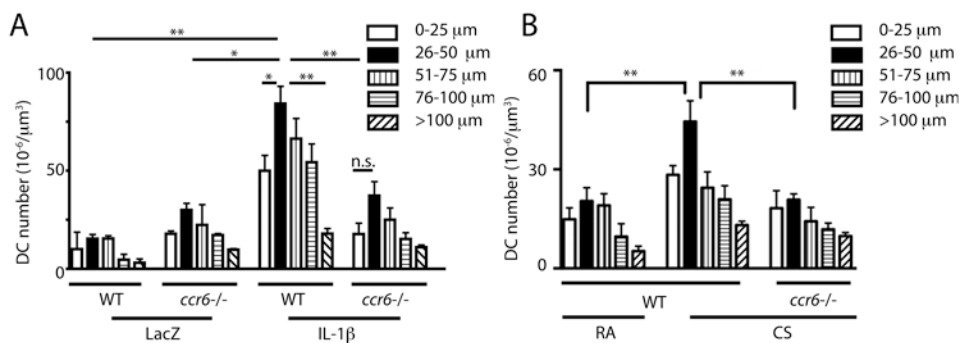


Fig. 3. *ccr6* is required for DC accumulation around airways in Ad-IL-1 β - and cigarette smoke (CS)-treated mice

2-photon microscopy of living vibratome lung sections of transgenic mice (Tg) expressing YFP under control of the CD11c promoter (in DCs and alveolar macrophages). CD11c-YFP mice were crossed to either WT (A,B) or *ccr6* deficient (*ccr6* -/-) mice. $N = 3$ mice in LacZ control and $N = 6$ in Ad-IL-1 β treated groups. Mice were treated either with intratracheal (IT)-Ad-LacZ, Ad-IL-1 β (A), room air (RA) or whole body cigarette smoke (CS) (B). Lung sections were harvested from mice 9 days after Ad-LacZ or Ad-IL-1 β 16 days after the initiation of smoke exposure. Images were analyzed using an automated imaging analysis software (IMARIS) which discriminates dendritic cells (DCs) from alveolar macrophages (AMs) based on sphericity. DCs were counted in predefined airway adjacent regions (0-25, 26-50, 51-75, 76-100 and >100 μ m from the airway lumen. $N=3$ in control groups and at least 6 in treatment groups from at least 3 independent experiments. * $p<0.05$, ** $p<0.01$, *** $p<0.001$ by ANOVA and Bonferroni's post-test.

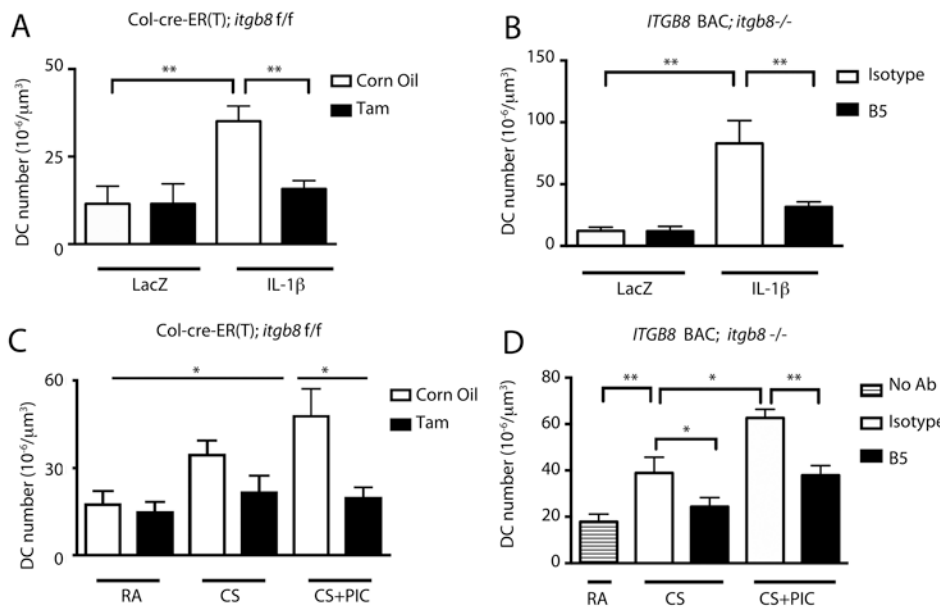


Fig. 4. $\alpha v \beta 8$ -expression by fibroblasts is required for DC accumulation around airways in Ad-IL-1 β -cigarette smoke (CS)- and CS plus poly (I:C)-treated mice

2-photon microscopy of living vibratome lung sections of transgenic mice (Tg) expressing YFP under control of the CD11c promoter (in DCs and alveolar macrophages). CD11c-YFP mice were crossed to col-cre-ER(T); *itgb8* f/f (A, B) or humanized $\beta 8$ Tg (BAC *ITGB8* Tg; *itgb8* -/-) mice (C, D). Col-cre-ER(T); *itgb8* f/f will specifically delete $\beta 8$ expression on lung fibroblasts in the presence of tamoxifen (Tam) (50). Each of these compound mouse strains were treated either with intratracheal (IT)-Ad-LacZ (A, C), Ad-IL-1 β (A, C) and harvested after 9 days, 16 days of whole body cigarette smoke (CS) (B, D), or 16 days of whole body CS in combination with intranasal poly I:C (CS+PIC) (B, D). IT-Ad-IL-1 β -mediated DC accumulation (<100 μ m) is dependent on fibroblast expression of $\alpha v \beta 8$ since it can be blocked by ligand-dependent (Tam) deletion of $\beta 8$ on fibroblasts (A) or neutralizing anti- $\beta 8$ antibody (B5) (C). DC accumulation (<100 μ m) in response to CS or CS-poly(I:C) is similarly blocked by ligand-dependent deletion of $\beta 8$ on fibroblasts (B) or B5 or D. N 3 mice in control, N 6 in IL-1 β treated, N 4 in CS-, CS-PIC treated Col-cre-ER(T); *itgb8* f/f mice or *ITGB8* BAC mice from at least 3 independent experiments. * p <0.05, ** p <0.01, *** p <0.001 by ANOVA and Bonferroni's post-test.

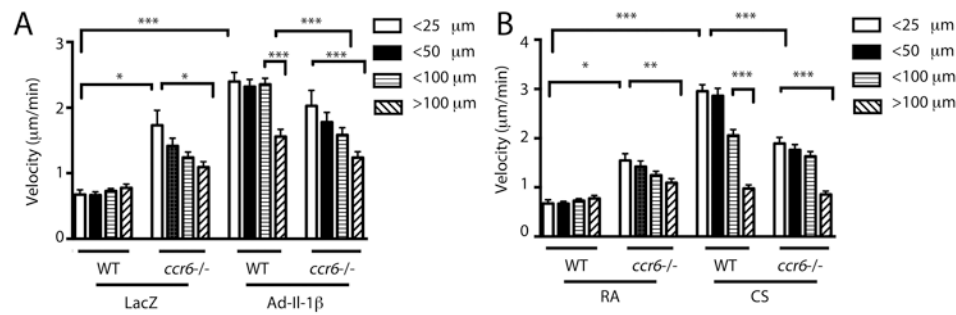


Fig. 5. Increased chemokinesis around small airways in mice treated with IL-1 β or cigarette smoke is dependent on *ccr6*

2-photon microscopy of living vibratome lung sections of CD11c-YFP mice crossed to either WT or *ccr6*^{-/-} mice. Mice were treated either with intratracheal (IT)-Ad-LacZ, Ad-IL-1 β (A) and harvested after 9 days, or B) room air (RA) or 16 days of whole body cigarette smoke (CS). DC velocity in mice treated with Ad-IL-1 β or CS by zone around airways (<25, <50, <100 or >100 μ m from the airway lumen) is dependent on *ccr6* since it is significantly decreased by deficiency of *ccr6*. $N=3$ mice in control and $N=3$ in IL-1 β and CS-treated *ccr6*^{-/-} groups from at least 3 independent experiments. * $p<0.05$, ** $p<0.01$, *** $p<0.001$ by ANOVA and Bonferroni's post-test.

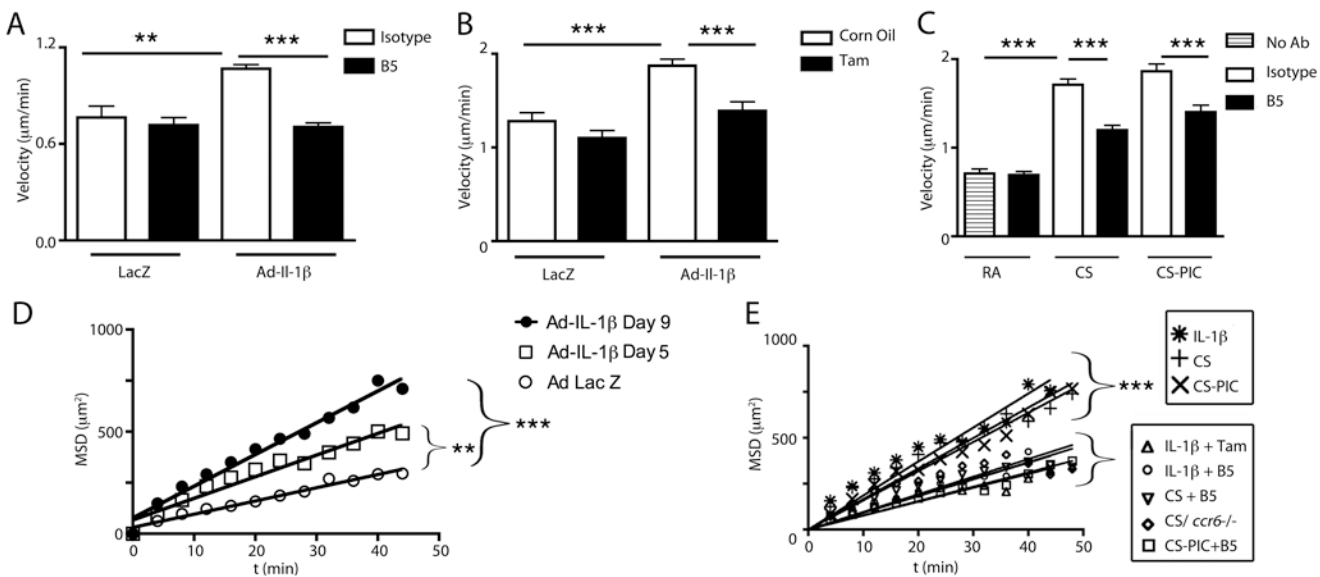


Fig. 6. Increased chemokinesis around small airways in mice treated with IL-1 β , cigarette smoke (CS) or CS-poly(I:C) is dependent on α v β 8-expression by fibroblasts

2-photon microscopy of living vibratome lung sections of CD11c-YFP mice crossed to BAC *ITGB8* Tg; *itgb8*-/- (A, C, D), Col-cre-ER(T);*itgb8f/f* (B, D), or *ccr6* -/- mice (D). Each of these compound mouse strains were treated either with intratracheal (IT)-Ad-LacZ, Ad-IL-1 β (A, B, D) and harvested after 9 days, room air (RA) or 16 days of whole body cigarette smoke (CS), or 16 days of whole body CS in combination with intranasal poly I:C (CS + PIC) (C, D). IT-IL-1 β -mediated increased DC velocity (<100 μ m) is dependent on fibroblast expression of α v β 8 since it can be blocked by (A) neutralizing anti- β 8 antibody (B5) or (B) ligand-dependent deletion of β 8 on fibroblasts. C) Increased DC velocity (<100 μ m) in response to CS or CS+poly I:C (PIC) is blocked by B5. D) Mean square displacement (MSD, μ m 2) plots vs. time for mice at day 5 vs. day 9 post-treatment with IT-Ad-IL-1 β . As a control, MSD vs. time plots for mice 5 days post-Ad-LacZ, are shown. All points fall on straight lines using linear regression, indicating random movement. The slope (motility coefficient) is greater for the groups treated with IT-Ad-IL-1 β compared with the Ad-LacZ group. $N=3$ mice in control and $N=3$ in IL-1 β treated mice from at minimum of 3 independent experiments. ** p <0.01, *** p <0.001 E) Mean square displacement (MSD, μ m 2) plots vs. time for all mouse groups. All points fall on straight lines indicating random movement. The slope (motility coefficient) is greater for the groups treated with IT-Ad-IL-1 β , CS or CS-poly(I:C) compared with groups with antibody treatment, *ccr6* deficiency, or fibroblast deletion of β 8. $N=3$ mice in control and $N=3$ in IL-1 β and CS, CS-PIC treated *ccr6* -/-, *ITGB8*BAC, col-cre-ER(T);*itgb8* f/f mice, from at least 3 independent experiments. ** p <0.01, *** p <0.001 by linear regression, or ANOVA and Bonferroni's post-test for multiple comparisons.

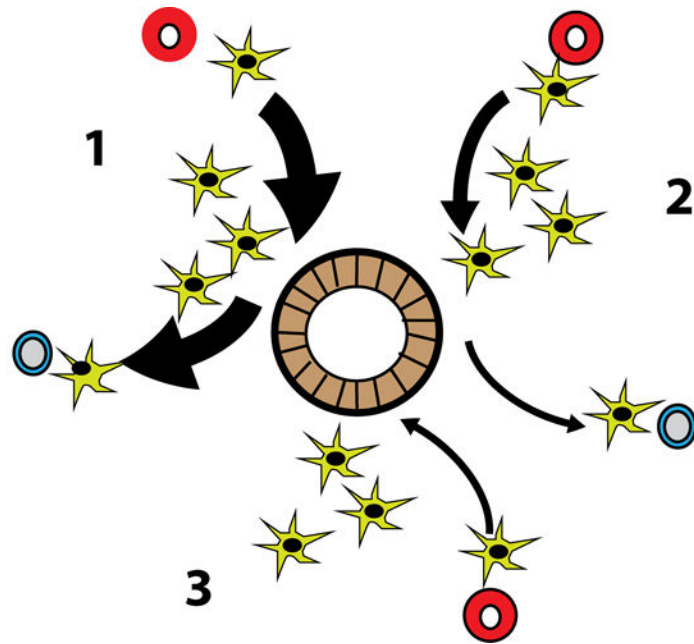


Fig. 7. Hypothetical mechanisms of increased DC accumulation around airways as detected using 2-photon microscopy

DCs might accumulate around airways by a number of mechanisms, alone or in combination. These mechanisms include: **1**) increased chemokinesis, **2**) increased local retention, or **3**) decreased emigration. **1**) Balanced increases in both immigration and emigration (**arrow**) from blood vessels (red) to lymphatics (blue) would be manifested by increased chemokinesis without detectable bulk directional migration (linearity in mean square displacement (MSD) vs. time.). **2**) Imbalanced chemokinesis during immigration (**wide arrow**) from vessels (red) and emigration (**narrow arrow**) to lymphatics (blue) would be manifested by increased chemokinesis with small changes in directionality as manifested by slight non-linearity in MSD vs. time. **3**) Pure chemotaxis would be manifested also by increased chemokinesis (**narrow arrow**) but with major changes in non-linearity in MSD vs. time plots.